Purification of Single-Walled Carbon Nanotubes Using a Supercritical Fluid Extraction Method

ARTICLE *in* THE JOURNAL OF PHYSICAL CHEMISTRY C · AUGUST 2007

Impact Factor: 4.77 · DOI: 10.1021/jp073374o

Purification of Single-Walled Carbon Nanotubes Using a Supercritical Fluid Extraction Method

Joanna S. Wang,[†] Chien M. Wai,*[,†] Kenichi Shimizu,[†] Frank Cheng,[†] John J. Boeckl,[‡] Benji Maruyama,[‡] and Gail Brown[‡]

Department of Chemistry, University of Idaho, Moscow, Idaho 83844, and Materials and Manufacturing Directorate, Air Force Research Laboratory, WPAFB, Ohio 45433

Received: May 2, 2007; In Final Form: June 12, 2007

Metal catalyst used in the production of single-walled carbon nanotubes (SWNTs) can be effectively removed from the as-grown nanotubes by an in situ chelation/supercritical fluid carbon dioxide extraction method. A pretreatment procedure using bulk electrolysis with ethylenediaminetetraacetic acid significantly improves the efficiency of supercritical fluid extraction probably by removing the amorphous carbon associated with the metal from the SWNTs. More than 98% of the iron impurity can be removed from the as-grown SWNTs using this two-step purification method without obvious damage to the nanotube structures according to our spectroscopic data.

1. Introduction

Since their discovery in the 1990s,[1,2] single-walled carbon nanotubes (SWNTs) have attracted a great deal of attention due to their unique physical, chemical, and mechanical properties.[3−7] SWNTs are expected to have potential applications in many areas, including field emission displays, supercapacitors, molecular computers, and ultra-high-strength carbon composite materials. To obtain optimal performance of SWNTs in various applications, high-purity SWNTs are required. The impurities in SWNTs typically are amorphous carbon and transition metals used as catalysts in the preparation and the growth of the CNTs. For example, in the HiPco process of synthesizing SWNTs, the disproportionation reaction $CO + CO \rightarrow C + CO_2$ is catalyzed by the zerovalent iron from the precursor $Fe(CO)_5$.[8,9] The iron catalyst is present as nanometer-sized particles on the surfaces of the synthesized SWNTs in transmission electron microscopy (TEM) as shown in Figure 1a.

Various purification methods for SWNTs have been reported in the literature including acid washing, gas-phase oxidation, electrochemical oxidation, ultrasonically assisted filtration, and microfiltration.[10−22] Tedious and time-consuming processes are often involved in these cleaning methods. For example, Hou et al.[10] reported a procedure for cleaning SWNTs, which included (1) ultrasonication for 30−80 min, (2) boiling in water at 100 °C for 50 h, (3) oxidizing at a temperature of 490−600 °C for 15−30 min, (4) immersing in 37% HCl until the solution became colorless, (5) washing with deionized water until the solution pH = 7, and (6) drying in an oven at 150 °C for 12 h. Chiang et al.[8,18] reported a two-stage purification process involving oxidation of SWNTs in an O_2/Ar atmosphere at two different temperatures with each oxidation step followed by a sonication wash with concentrated HCl. A cyclic volumetric (CV) oxidation method for SWMTs in a KOH solution was investigated by Fang et al.[17] After 80 cycles of CV oxidation, amorphous carbon in the as-grown SWNTs was effectively removed, leading to the exposure of metal nanoparticles, hence facilitating the removal of the metal impurities by subsequent HCl washing. Dillon et al.[21] refluxed raw SWNTs in 3 M HNO_3 for 16 h at 120 °C; after that the solids were collected on a polymer filter and rinsed with deionized water. Generally speaking, current methods for purification of SWNTs usually involve multisteps including chemical or electrochemical oxidation, sonication, and acid dissolution at elevated temperatures.

Supercritical fluid carbon dioxide (Sc-CO_2) has been shown to be an effective solvent for removing organic and inorganic substances from porous solid materials. Sc-CO_2 has both gaslike and liquidlike properties; thus, it can penetrate into small pores like a gas and dissolve organic substances like a liquid. After dissolution, Sc-CO_2 can be rapidly removed from the system by pressure reduction with minimal liquid waste generation. Several recent reports have demonstrated that transition metals in solid materials can be effectively extracted using Sc-CO_2 containing a proper oxidizing agent and a chelating agent at moderate temperatures.[23−28] In this paper, we present our initial results of cleaning metal impurities from as-grown SWNTs produced by the HiPco process using Sc-CO_2 as a solvent. The whole purification process involves two steps, a pretreatment step and a supercritical fluid extraction step. Up to 98% of the initial metal in the as-grown SWNTs can be removed using this method. The purification procedure and characterization of the SWNTs before and after the treatment are given in this paper.

2. Experimental Section

2.1. Reagents and Apparatus. The as-grown SWNTs were obtained from CNI (Carbon Nanotechnologies, Inc., Houston, TX). Instrument-grade CO_2 (99.99% purity) (Airgas, Dayton, OH) was used in all experiments. Tri-*n*-butyl phosphate (TBP), thenoyltrifluoroacetylacetone (TTA), HFA (hexafluoroacetylacetone), and hexanes were obtained from Aldrich (Aldrich Chemical Co., Milwaukee, WI). Deionized water (Millipore Milli-Q system, Bedford, MA) was used for the preparation of aqueous solutions. Disodium ethylenediaminetetraacetate dihy-

* To whom correspondence should be addressed. E-mail: cwai@uidaho.edu. Phone: (208) 885-6787. Fax: (208) 885-6173.
† University of Idaho.
‡ Air Force Research Laboratory.

10.1021/jp073374o CCC: $37.00
Published on Web 08/10/2007

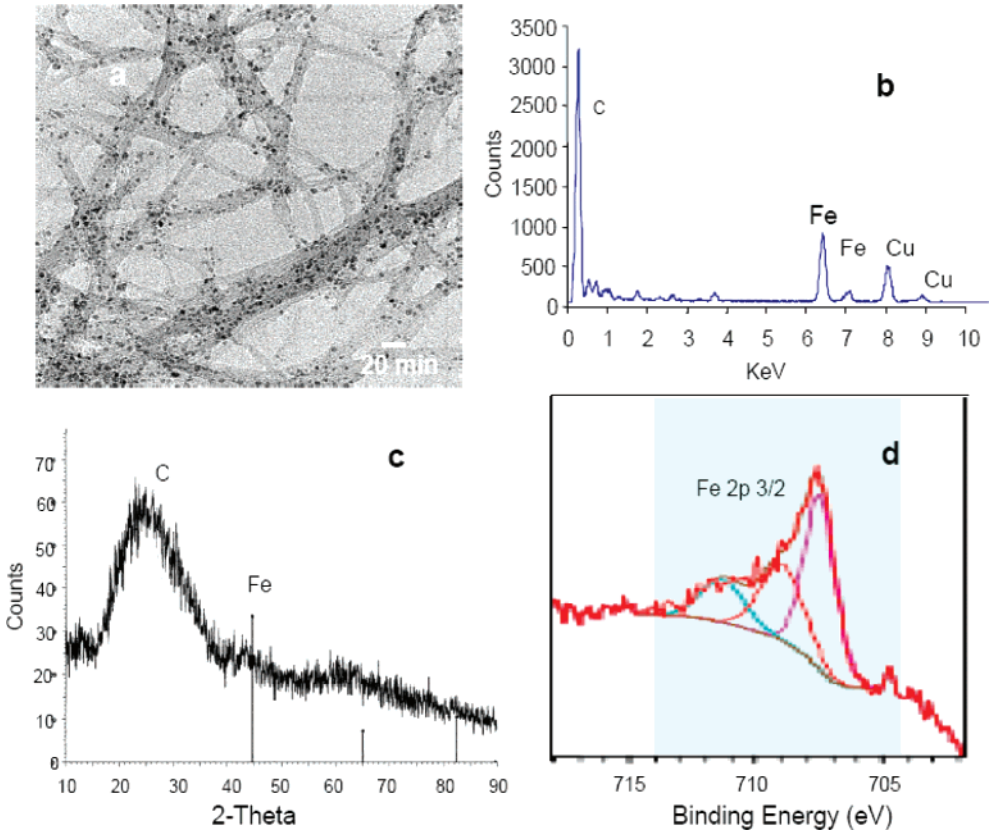

Figure 1. (a) TEM image of the as-grown SWNTs, (b) EDS of the as-grown SWNTs, (c) XRD of the as-grown SWNTs, and (d) XPS of the as-grown SWNTs.

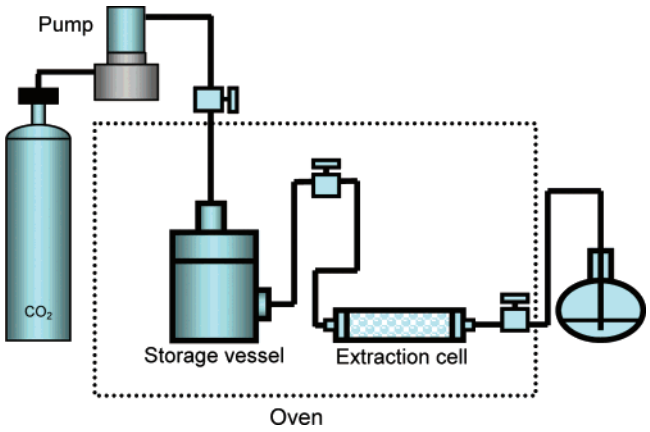

Figure 2. SFE apparatus for metal impurity removal from SWNTs.

drate (EDTA; 100%) was obtained from J. T. Baker. A 16-mL platinum (Pt) crucible, which was used as the sample container as well as the working electrode in bulk electrolysis, was cleaned with concentrated hydrochloric acid (ACS grade, EMD) before use. A Pt wire used as the auxiliary electrode was obtained from Aldrich (99.99%), and a Ag/AgCl (3 M KCl) reference electrode was obtained from Bioanalytical Science (BASi, West Lafayette, IN). Ethanol was of ACS/USP grade from AAPER Alcohol and Chemical Co. (Shelbyville, KY).

The high-pressure apparatus for supercritical fluid extraction (SFE) of metal species is described in the literature.[23] The apparatus for the SFE experiments basically includes a liquid CO_2 tank, a high-pressure syringe pump, an extraction cell, and a collection vial as shown in Figure 2. SFC-grade CO_2 was delivered to the extraction system with a syringe pump (ISCO, model 260D, Lincoln, NE) with a controllable pressure and flow rate. The experiments were performed with a stainless steel extraction vessel (6.94 mL) maintained at a desired temperature by placing it in a thermostat oven. The pore size of the frits at both ends of the vessel was 0.5 μm.

A CO_2-soluble nitric acid complex of the formula (TBP)-$(HNO_3)_{1.8}(H_2O)_{0.6}$ was prepared by shaking TBP with concentrated nitric acid according to the procedure given in the literature.[24,27] Because TBP is highly soluble in Sc-CO_2, it can bring a CO_2-insoluble inorganic acid such as nitric acid into Sc-CO_2 in the form of a Lewis acid−base complex for oxidation and dissolution of metals and metal oxides. Sc-CO_2 extraction conditions were set for 90 min of static extraction, followed by a 30 min dynamic extraction using neat CO_2 at 60 °C and 200 atm in a thermostatically controlled oven. At the oven exit, a stainless steel tube (316 SS, 1/16 in. o.d. and 0.030 in. i.d.) approximately 20 cm in length was used as the pressure restrictor for the exit CO_2. After depressurizing, the CNTs were removed from the cell by washing with a small amount of methanol. The SWNTs in the methanol solution were centrifuged, washed with methanol several times, and then collected and dried at a temperature around 70 °C for characterization.

A sonicator (Col Parmer, Vernon Hills, IL) with powers of 160 W (input) and 70 W (output) at a frequency of 42 kHz was used in the pretreatment process. TEM images of the SWNTs were taken using a Jeol TEM 2010 microscope equipped with an Oxford ISIS system. To obtain TEM images, the SWNTs were dispersed in ethanol under ultrasonication for 1 min and were then deposited on a carbon-coated copper grid. Energy-dispersive X-ray spectroscopy (EDS) was performed using a LEO SUPRA 35 VP (FESEM). Power X-ray diffraction (XRD) patterns of the SWNTs were obtained using a Siemens D5000 instrument. X-ray photoelectron spectroscopy (XPS) was performed using a Kratos AXIS-165 instrument with an Al Kα source.

Raman spectra were collected with a Raman spectrometer (Renishaw InVia Raman microscope) using a HeNe laser (633 nm) at a laser power of ~0.068 mW with one data accumulation and a detector data acquisition time of ~10 s. A piece of a silicon wafer was carefully rinsed by acetone and by methanol, followed by addition of one drop of a methanol/SWNT solution to the substrate surface. The samples so prepared were used for Raman spectroscopic measurements.

2.2. Electrolysis Procedure. A few milligrams of the as-grown SWNTs were placed in a Pt crucible, and about 0.1 mL of a water/ethanol mixture (1:1, v/v) was quickly added afterward to keep the SWNTs from scattering in the air. A 5 mL sample of an electrolyte solution, consisting of 0.5 M KCl and 5 mM EDTA, was added to the Pt crucible. EDTA was added to facilitate dissolution of iron due to the strong Fe(II)−EDTA complex formation in aqueous solution. The bulk electrolysis was conducted using a Bioanalytical Systems (BASi) CV-50w potentiostat (West Lafayette, IN) and a three-electrode cell, i.e., the Pt crucible working electrode, a Ag/AgCl reference electrode, and a Pt wire auxiliary electrode. The applied potential was set at 0.4 $V_{Ag/AgCl}$, which is more positive (oxidative) than the standard reduction potential of iron (eq 1), so that the current

$$Fe^{2+} + 2e^- = Fe^0 \qquad E^0 = -0.44\ V_{NHE} \text{ or } -0.23\ V_{Ag/AgCl} \quad (1)$$

depends only on the mass transfer.[29] Bulk electrolysis took place for approximately 1 h (4000 s). Since our electrochemical cell was open to the atmosphere, we must consider the presence of dissolved oxygen, which is also an electroactive element (eq 2). At 0.40 $V_{Ag/AgCl}$, the electrochemical cell does not require

$$O_2 + 2H_2O + 4e^- \rightarrow 4OH^- \qquad E^0 = +0.40\ V_{NHE} \text{ or } +0.61\ V_{Ag/AgCl} \quad (2)$$

deoxygenation to avoid the current generated by the reduction of dissolved oxygen. For this reason, the bulk electrolysis was carried out at 0.40 $V_{Ag/AgCl}$ for 1 h under atmospheric conditions.

After the electrolysis, the SWNT mixture was transferred to a vial with trichloroethylene and placed in a centrifuge for 30 min. Trichloroethylene, with a density of 1.4 mg/mL, served as a medium to separate the SWNTs from the aqueous solution. The supernatant aqueous solution was carefully pipetted out from the vial after the centrifugation, and then methanol was added to the remaining SWNTs to wash off trichloroethylene. The SWNTs were washed with methanol several times and dried under atmospheric conditions for SFE experiments.

3. Results and Discussion

3.1. Spectroscopic Characterization of the Metal Impurity in SWNTs. The X-ray diffraction pattern of the as-grown SWNTs used in this study reveals no distinct peaks of iron as shown in Figure 1c even though EDS shows the presence of iron (Figure 1b). The iron present in the as-grown SWNTs probably does not have crystal structures. The XPS spectrum of the SWNTs shows the presence of iron species with different oxidation states including Fe^0, Fe(II), and Fe(III). The oxidized iron peaks can be fitted into FeO and Fe_2O_3 as shown in Figure 1d. The distribution of the iron species in the SWNTs appears to depend on the shelving time. A newly obtained sample from Carbon Nanotechnologies, Inc. showed about 60% zerovalent iron and 40% divalent iron. Another SWNT sample from the same supplier with a longer shelving time showed 50% zerovalent iron, 35% divalent iron, and 15% trivalent iron according to the XPS spectra.

It is known that amorphous carbon is present in the SWNTs and the iron impurity may be covered by the amorphous carbon. Our initial SFE experiments indicate that, without a pretreatment step, about 60% of the Fe in the as-grown SWNTs could be removed by one cycle of the SFE treatment. Repeated Sc-CO_2 extraction would not significantly improve the removal of Fe from the SWNTs. Presumably this fraction of hard-to-remove Fe impurity is associated with the amorphous carbon present in the system. It appears necessary to remove the amorphous carbon in the SWNTs to expose all iron impurity for their subsequent extraction by Sc-CO_2. On the basis of the initial SFE results, we decided to use a pretreatment step prior to the SFE for purification of the as-grown SWNTs. Two pretreatment procedures were tested. One procedure is use of a sonication-assisted acid dissolution, and the other is bulk electrolysis using EDTA as a complexing agent.

3.2. Pretreatment with Acid/Sonication Followed by SFE. In this procedure, an SWNT sample was placed in a small vial subjected to a sonication step with $(TBP)(HNO_3)_{1.8}(H_2O)_{0.6}$ at 45 °C for 1.5 h. After that, the SWNT sample was transferred to the high-pressure extraction cell and extracted by Sc-CO_2 containing a mixture of $(TBP)(HNO_3)_{1.8}(H_2O)_{0.6}$ and a fluorinated β-diketone such as HFA or TTA at 60 °C and 200 atm for 1.5 h. It is known that HFA and TTA form stable chelates with a number of transition-metal ions that are highly soluble in Sc-CO_2. A mixture of $(TBP)(HNO_3)_{1.8}(H_2O)_{0.6}$ and TTA has been used to dissolve lanthanide oxides, uranium dioxide, and transition metals in Sc-CO_2.[23−28] The mechanism probably involves dissolution and oxidation of metal species by the acid followed by formation of metal β-diketonates that become soluble in Sc-CO_2. The static extraction is followed by 30 min of dynamic flushing to remove the dissolved iron β-diketonate from the system. After the SFE, TEM images of the treated SWNTs showed only a few metallic nanoparticles on their surfaces (Figure 3b). EDS data indicated that the percent of Fe in the SWNT sample was reduced from about 30% (w/w) in "as-grown" SWNTs to about 0.5% (w/w) after the SFE process with a total metal removal of over 98%. Figure 3d shows the EDS spectra of the SWNTs after the hyphenated pretreatment−SFE process using HFA as the chelating agent. When the chelating agent TTA was used, a peak of S located around 2.3 keV usually showed up which probably came from the residue of the chelating agent. When HFA was used, this S peak was not detectable. The solubility of HFA in Sc-CO_2 is about 2 orders of magnitude higher than that of TTA and is better for the dissolution and chelation of metal cations. On the other hand, TTA is often used in SFE of metals because it is a solid at room temperature and is easier to handle than other liquid fluorinated β-diketones in SFE experiments. TEM images also showed that in the presence of a surfactant sodium dodecyl sulfate (SDS) in the pretreatment step assisted untangling of the SWNTs.

3.3. Pretreatment with Bulk Electrolysis Followed by SFE. Bulk electrolysis is a controlled-potential method in which the applied potential is kept constant during analysis. It is a desirable electrochemical method to complete an electrolytic process in a solution. Figure 4 shows the current−time curve generated as a result of the bulk electrolysis of the solution containing the SWNTs and 0.5 M KCl with (upper line) and without (lower line) 5 mM EDTA. The curve with the presence of EDTA showed significantly higher current generation than that without EDTA after 1 h of electrolysis. The higher current indicates an

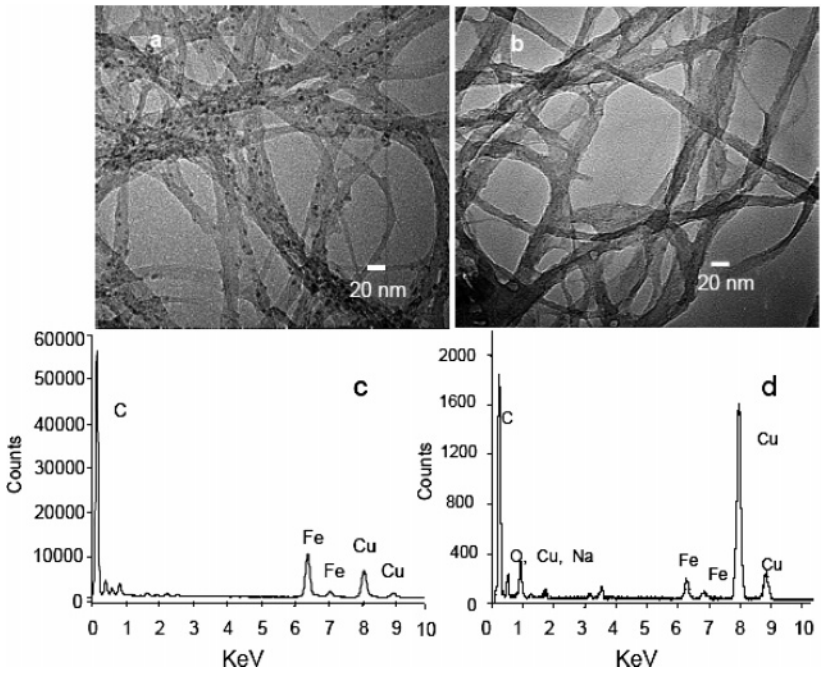

Figure 3. (a) TEM image of SWNTs pretreated by acid/sonication using $(TBP)(HNO_3)_{1.8}(H_2O)_{0.6}$ as an acidic medium at 45 °C, (b) TEM image after the acid pretreatment and SFE, (c) EDS spectrum of SWNTs after pretreatment by acid/sonication, and (d) EDS spectrum after acid pretreatment and SFE.

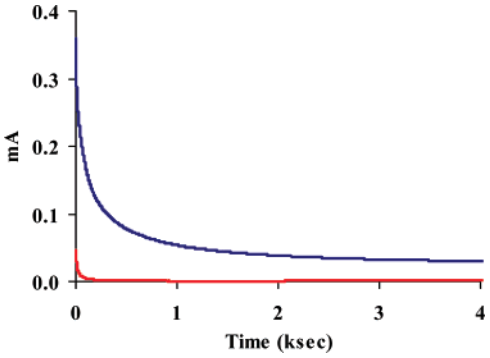

Figure 4. Current versus time curve generated by the bulk electrolysis, which was undertaken in the solution containing 2 mg of SWNTs and 0.5 M KCl. The upper line is with 5 mM EDTA, and the lower line is without EDTA in the solution. The electrode potential was at 0.40 V vs Ag/AgCl (reference electrode).

enhanced dissolution of iron in the system which is attributed to the Fe(II)−EDTA complex formation shown in eq 3. Using the EDTA complex formation technique, the currents associated with nonfaradic processes, i.e., the solvent adsorption onto the SWNTs, are probably small.

$$Fe^{2+} + EDTA^{4-} = Fe^{II}EDTA^{2-} \qquad K = 10^{14.32} \qquad (3)$$

The redox current was observed at 0.3 mA when voltage was applied at the starting point of the bulk electrolysis as shown in Figure 4. After 30 min, the current remained nearly constant at 0.05 mA and stayed almost constant until the end of the electrolysis. The current from the bulk electrolysis is probably an indication of the efficiency of removal of the amorphous carbon and the Fe impurity from the SWNTs. The current response was nearly constant once the removal of the impurities by the electrolysis was completed. At the end of the electrolysis, the current response was much higher from the EDTA solution than from that without EDTA. This suggested that some electrochemical processes were still in progress. This could be attributed to the electrolysis-generated products such as Fe^{II}-EDTA, which was electrochemically oxidized to $Fe^{III}EDTA$ as shown in eq 4.

$$Fe^{III}EDTA + e^- = Fe^{II}EDTA \qquad E^0 = -0.11\ V_{Ag/AgCl} \qquad (4)$$

Figure 5a shows the EDS spectrum of the SWNTs after the electrolysis for 1 h in the presence of EDTA. The iron peak at 6.5 keV is significantly reduced (50−60%) after the electrolysis. The TEM image of the SWNTs also shows fewer iron particles on the surfaces (Figure 5d). In the absence of EDTA, EDS data and TEM images of the SWNTs after the electrolysis show only a small reduction of iron particles (<10%) compared with the original sample.

After bulk electrolysis, the SWNTs were treated by Sc-CO_2 extraction under the same conditions described in the previous section. After SFE, the overall removal of the Fe impurity was >98% (Figure 5b) according to the EDS result. TEM images are supportive of this result (Figure 5d). Using HFA as a chelating agent, the TEM images show that the SFE efficiency to remove the catalytic metal impurity is better compared with that of TTA. The electrolysis pretreatment conditions were mild, and the SWNTs after the pretreatment showed little change in structure as indicated by our Raman spectroscopy study.

3.4. Raman Spectra of SWNTs. SWNTs have distinct Raman features[30,31] that can be used to characterize the material. Specifically, the D, G, and G′ bands around 1330, 1600, and 2700 cm^{-1}, respectively, are related to graphitic carbon and carbon nanotubes.[30] In the range around 1600 cm^{-1}, SWNTs typically show a characteristic double peak structure. The double-resonant Raman scattering arises from the peculiar electronic band structure of SWNTs. The radial breathing modes around 200 nm can be correlated to the nanotube diameter by the relationship d (diameter) = (234 nm)/ν, where ν is the wavenumber of the peak.[8,18]

Figure 6 shows the Raman spectra of the as-grown and the treated SWNT samples in the range 100−3200 cm^{-1} taken with a 633 nm laser excitation. The spectra show typical SWNT

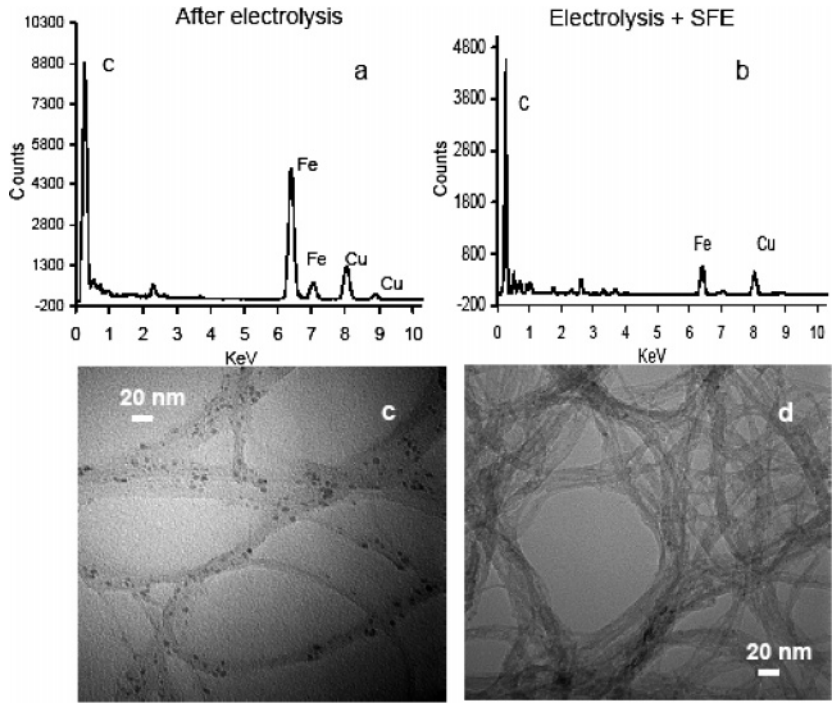

Figure 5. (a) EDS spectra of SWNTs after electrolysis and (b) after electrolysis/SFE and (c) TEM images after electrolysis and (d) after electrolysis/SFE.

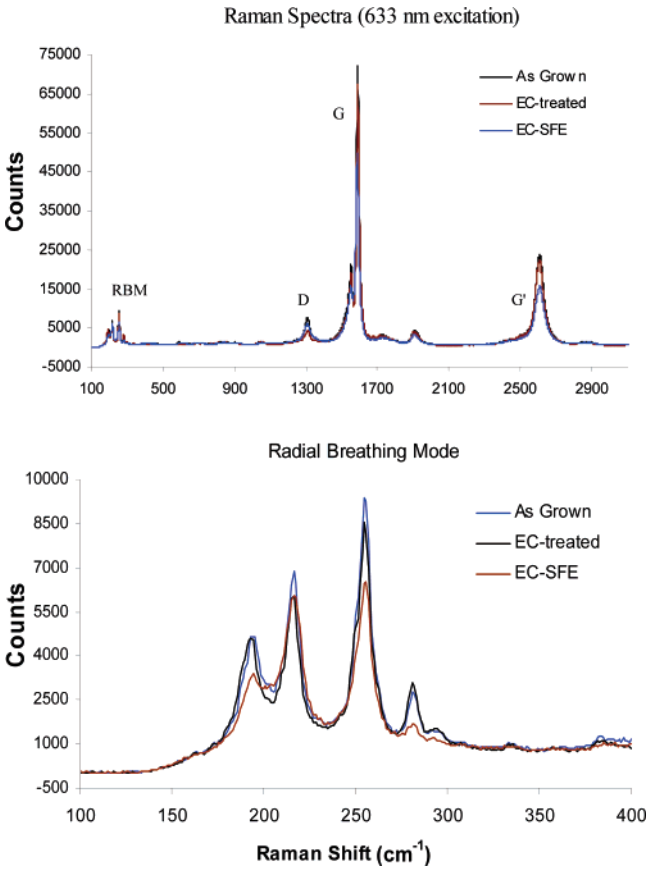

Figure 6. Top: Raman spectra of SWNTs (633 nm excitation). Bottom: RBM of the Raman spectra.

features for the tangential carbon stretching modes (G lines) around 1600 cm^{-1} and radial breathing modes (RBMs) in the region of 200 cm^{-1}.[8,18,32] The as-grown and after electrolysis SWNT samples show very little change in their Raman spectra, indicating the structures of SWNTs remain basically intact after electrolysis. However, SWNTs treated by acid/sonication showed a decrease in intensity of the radial breathing modes by a factor of 2 relative to the as-grown sample, which could be attributed to defects created during the acid pretreatment. The decrease in Raman intensity in both the tangential and radial modes was reported in the literature using oxidation and HCl sonication for purification of SWNTs.[8,18] After the supercritical fluid extraction, the intensity of the radial breathing modes showed a decrease in intensity by about 30% for the most intense peak at 255 nm and to a greater extent for the small peak at 285 nm. The tangential stretching modes showed little change after the supercritical fluid extraction. Generally speaking, the decrease in Raman intensities using our purification method is small compared with that reported by Chiang et al. using oxidation and HCl sonication for purification of SWNTs.[18] These authors also showed that, by annealing the purified SWNTs at 800 °C in Ar, the Raman peak intensities would increase after the heat treatment.

4. Conclusions

Supercritical fluid extraction combined with a pretreatment procedure provides an effective way of removing the iron impurity from as-grown SWNTs synthesized by the HiPco process. XPS spectroscopy indicates that the iron impurity in the SWNTs consists of zerovalent iron and iron oxides. Pretreatment of the SWNTs by bulk electrolysis in the presence of EDTA enhances the efficiency of iron extraction by Sc-CO_2 probably due to removal of amorphous carbon that covers the metallic iron impurity. The SFE process proceeds at 60 °C and 200 atm using a nitric acid complex and a β-diketone as extractants. Over 98% of the iron impurity in the as-grown SWNTs can be removed using this two-step extraction process. Raman spectroscopy suggests the structure of the SWNTs remains basically intact after the electrolysis/SFE purification process. An acid/sonication pretreatment in combination with SFE can also remove over 98% of the iron impurity in the SWNTs. However, the acid pretreatment may result in structure damage to the SWNTs. In principle, the supercritical fluid extraction method described in this paper should be able to

remove other metal impurities present in SWNTs synthesized by different methods. Further research along this direction is currently in progress.

Acknowledgment. This work was supported by the AFOSR (Grant FA9550-06-1-0526).

References and Notes

(1) Iijima, S.; Ichihashi, T. *Nature* **1993**, *363*, 603.
(2) Iijima, S.; Ichihashi, T. *Nature* **1993**, *364*, 737.
(3) Issi, J. P.; Langer, L.; Heremans, J.; Olk, C. H. *Carbon* **1995**, *33*, 941.
(4) Cornwell, C. F.; Wille, L. T. *Solid State Commun.* **1997**, *101*, 555.
(5) Fuhrer, M. S.; Nygard, J.; Shih, L.; Forero, M.; Yoon, Y. G.; Mazzoni, M. S.; Zetti, A.; McEuen, P. *Science* **2000**, *288*, 494.
(6) Rosen, R.; Simendinger, W.; Debbault, C.; Shimoda, H.; Stoner, L.; Zhou, O. *Appl. Phys. Lett.* **2000**, *76*, 1668.
(7) Smith, B. W.; Luzzi, D. E. *Chem. Phys. Lett.* **2000**, *32*, 169.
(8) Chiang, I. W.; Brinson, B. E.; Huang, A. Y.; Willis, P. A.; Bronikowski, M. J.; Margrave, J. L.; Smalley, R. E.; Hauge, R. H. *J. Phys. Chem. B* **2001**, *105*, 8297.
(9) Nikolaev, P.; Bronikowski, M. J.; Bradley, R. K.; Rohmund, F.; Colbert, D. T.; Smith, K. A.; Smalley, R. E. *Chem. Phys. Lett.* **1999**, *313*, 91.
(10) Hou, P. X.; Liu, C.; Tong, Y.; Xu, S.; Liu, M.; Cheng, J. H. *J. Mater. Res.* **2001**, *16*, 2526.
(11) Harutyunyan, A. R.; Prahan, B. K.; Chang, J.; Chen, G.; Eklund, P. C. *J. Phys. Chem. B* **2002**, *106*, 8671.
(12) Chattopadhyay, D.; Galeska, I.; Padadimitrakopoulos, F. *Carbon* **2002**, *40*, 985.
(13) Rinzler, A.; Liu, J.; Dai, H.; Nikolaev, P.; Huffman, C.; Rodriguez-Macias, F.; Boul, P.; Lu, A.; Heymann, D.; Colbert, D. T.; Lee, R. S.; Fischer, J.; Rao, A.; Eklund, P. C.; Smalley, R. E. *Appl. Phys. A* **1998**, *67*, 29.
(14) Tohji, K.; Takahashi, H.; Shinoda, Y. *J. Phys. Chem. B* **1997**, *101*, 1974.
(15) Zimmerman, J. L.; Bradley, R. K.; Huffman, C. B.; Hauge, R. H.; Margrave, J. L. *Chem. Mater.* **2000**, *12*, 1361.
(16) Jeong, T.; Kim, W.-Y.; Hahn, Y.-B. *Chem. Phys. Lett.* **2001**, *344*, 18.
(17) Fang, H.-T.; Liu, C.-G.; Liu, C.; Li, F.; Liu, M.; Cheng, H.-M. *Chem. Mater.* **2004**, *16*, 5744.
(18) Chiang, I. W.; Brinson, B. E.; Smalley, R. E.; Margrave, J. L.; Hauge, R. H. *J. Phys. Chem. B* **2001**, *105*, 1157.
(19) Shelimov, K. B.; Esenaliev, R. O.; Rinzler, A. G.; Huffman, C. B.; Smalley, R. E. *Chem. Phys. Lett.* **1998**, *282*, 429.
(20) Bandow, S.; Rao, A. M.; Williams, K. A.; Thess, A.; Smalley, R. E.; Eklund, P. C. *J. Phys. Chem B* **1997**, *101*, 8839.
(21) Dillon, A. C.; Gennett, T.; Jones, K. M.; Alleman, J. L.; Parilla, P. A.; Heben, M. J. *Adv. Mater.* **1999**, *11*, 1354.
(22) Duesberg, G. S.; Burghard, M.; Muster, J.; Philipp, J.; Roth, S. *Chem. Commun.* **1998**, 435.
(23) Wang, J. S.; Koh, M. S.; Wai, C. M. *Ind. Chem. Eng. Res.* **2004**, *43*, 1580.
(24) Enokida, Y.; El-Fatah, S. A.; Wai, C. M. *Ind. Eng. Chem. Res.* **2002**, *41*, 2282.
(25) Tomioka, O.; Meguro, Y.; Yoshida, Z.; Enokida, Y.; Yamamoto, I.; Yoshida, Z. *J. Nucl. Sci. Technol.* **2001**, *38*, 1097.
(26) Samsonov, M. D.; Wai, C. M.; Lee, S. C.; Kulyako, Y.; Smart, N. G. *Chem. Commun*. **2001**, 1868.
(27) Enokida, Y.; Tomika, O.; Lee, S. C.; Rustenholtz, A.; Wai, C. M. *Ind. Eng. Chem. Res*. **2003**, *42*, 5037.
(28) Wang, J. S.; Wai, C. M. *Ind. Chem. Eng. Res.* **2005**, *44*, 922.
(29) Bard, A. J.; Faulkner, L. R. *Electrochemical Methods Fundamentals and Applications*; John Wiley and Sons: New York, 2001; p 417.
(30) Qian, W.; Liu, T.; Wei, F.; Yuan, H. *Carbon* **2003**, *41*, 1851.
(31) Coleman, J. N.; Maier, S.; Fleming, A.; O'Flaherty, S.; Minett, A.; Ferreira, M. S.; Hutzler, S.; Blau, W. J. *J. Phys. Chem. B* **2004**, *108*, 3446.
(32) Bandow, S.; Asaka, S.; Saito, Y.; Rao, A. M.; Grigorian, L.; Richter, E.; Eklund, P. C. *Phys. Rev. Lett.* **1998**, *80*, 3779.